# Numerical Modeling of Concrete Cylinders Confined with CFRP Composites

**Article** *in* Journal of Reinforced Plastics and Composites · August 2008
DOI: 10.1177/0731684407084212



3 authors:


Pedram Sadeghian
Dalhousie University



Alireza Rahai
Amirkabir University of Technology



Mohammad R. Ehsani
The University of Arizona

# Numerical modeling of concrete cylinders confined with CFRP composites

Pedram Sadeghian [a,*], Ali R. Rahai [a], Mohammad R. Ehsani [b]

[a] Department of Civil and Environmental Engineering, Amirkabir University of Technology
No. 424, Hafez St., Enghelab Av., Tehran, Iran

[b] Department of Civil Engineering and Engineering Mechanics, University of Arizona
Bldg. No. 72, Room 206, Tucson, AZ 85721, USA

[*] Corresponding author. Tel.: +98-912-200-2568; fax: +98-21-8879-6665
E-mail address: Pedsad@yahoo.com & Sadeghian@aut.ac.ir (P. Sadeghian)

## Abstract

This paper presents the results of numerical analyses of concrete cylinders (i.e. columns) confined in composites jackets. The specimens were subjected to uniaxial compression and the analysis was carried out using nonlinear finite element method. The various parameters such as wrap thickness, fiber orientation, concrete strength, interfacial bonding were considered. Three different wrap thicknesses (0.9, 1.8, and 2.7 mm), fiber orientation of $0^o$, $\pm 15^o$, $\pm 30^o$, and $\pm 45^o$ with respect to the hoop direction, and concrete strength values ranging from 20 MPa to 40 MPa were investigated. The finite element analysis results were in good agreement with experimental data presented by other researchers. The numerical analysis results demonstrated significant enhancement in the compressive strength, stiffness, and ductility of the CFRP-wrapped concrete cylinders as compared to unconfined concrete cylinders. The stress-strain response of cylinders was greatly affected by analysis parameters.

**Keywords:** Concrete column; strengthening; FRP; fiber orientation, confinement; ductility; finite element analysis.

## 1. Introduction

In recent years, Fiber Reinforced Polymer (FRP) composites have extensively been used in order to strengthen of concrete structures. The carbon FRP (CFRP) composites as unidirectional laminates are ideal materials for confining existing concrete columns. When the fiber-wrapped concrete is subjected to an axial compression loading, the concrete core expands laterally. This expansion is resisted by the FRP, and therefore the concrete core is changed to a three dimensional compressive stress state. In this state, performance of the concrete core is significantly influenced by the confinement pressure.

The confinement pressure provided by the FRP increases continuously with the lateral strain of concrete because of the linear elastic stress–strain behavior of FRP, in contrast to steel-confined concrete in which the confining pressure remains constant when the steel is in plastic flow. Failure of fiber-wrapped concrete generally occurs when the hoop rupture strength of the FRP is reached [1]. Several parameters influence the confinement effectiveness of FRP, which include concrete strength, wrap thickness or number of FRP layers, and wrap angle orientation [2].

Many investigations have been conducted into the behavior of fiber-wrapped concrete and as a result, a number of stress–strain models have been proposed. These models can be classified into two categories: (a) design-oriented models, and (b) analysis-oriented models. In the first category, the compressive strength, ultimate axial strain and stress–strain behavior of fiber-wrapped concrete are predicted using closedform equations based directly on the interpretation of experimental results. In the second category, stress–strain curves of fiber-wrapped concrete are generated using an incremental numerical procedure [3]. The present study is concentrated on the second category through a three-dimensional (3D) finite element (FE) modeling of CFRP wrapped concrete columns in uniaxial compression loading.

## 2. Background

The 3D numerical modeling of fiber-wrapped concrete columns is performed in order to develop a better understanding of nonlinear behavior of confined concrete in triaxial states of stress. In recent past substantial studies reported different approaches on the FE modeling of fiber-wrapped concrete columns. These studies have been mainly concentrated on the stress-strain response of fiber-wrapped concrete.

Parvin and Jamwal [2] investigated behavior of small-scale FRP-wrapped concrete cylinders in uniaxial compression loading through MARC [4] nonlinear FE analysis. Along with Mohr–Coulomb failure criterion, isotropic work hardening rule defined the concrete material's plastic behavior. Two parameters were considered for this numerical study: the wrap thickness, and the fiber orientation. Performances of numerical models with ''hoop-angle-hoop'' and ''angle-hoop-angle'' fiber orientations were compared, where the terms ''hoop'' and ''angle'' indicate that wraps were oriented at an angle of $0^{o}$ and $45^{o}$ in reference to hoop direction, respectively. For example, hoop-angle-hoop specimens were confined by wrapping the sample in three layers of FRP where the fibers in the two exterior layers were in the hoop direction and the fibers in the middle layer was inclined at 45 degrees.

The analysis results showed substantial increase in the axial compressive strength and ductility of the FRP-wrapped concrete cylinders as compared to the unconfined ones. The cylinders with ‘‘hoop-angle-hoop’’ fiber orientation in general exhibited higher axial stress and strain capacities as compared to the cylinders with the ‘‘angle-hoop-angle’’ fiber orientation. The increase in wrap thickness also resulted in enhancement of axial strength and ductility of the concrete cylinders.

Parvin and Jamwal [5] continued above parametric study for various fiber orientation, wrap thicknesses, and concrete strengths. Three different wrap thicknesses, fiber orientation of $0^o$, $\pm 15^o$, and $0^o/\pm 15^o/0^o$, and concrete strength values ranging from 3 ksi to 6 ksi (20.7 MPa to 41.4 MPa) were considered. The analysis results showed substantial increase in the axial compressive strength and ductility of the FRP-wrapped concrete cylinders as compared to the unconfined cylinders. The increase in wrap thickness also resulted in enhancement of axial strength and ductility of the concrete columns. The gain in axial compressive strength in FRP-wrapped concrete columns was observed to be higher for lower strength concrete and the highest in the columns wrapped with the $0^o$ fiber orientation.

Li et al. [6] conducted a parametric analysis using ANSYS [7] FE analysis, along with Willam-Warnke [8] failure criterion for FRP wrapped concrete. The effect of the thickness, stiffness, and fiber orientation of the wrap as well as the interfacial bonding between the wrap and the concrete on the strength and stiffness of the repaired columns was evaluated. Based on the parametric analysis, the stress-strain response was characterized by three distinct regions. There was a transition zone between the first region where the wrap is dormant and the third region where the wrap is fully activated. Increasing the interfacial bonding, the thickness, and the modulus of elasticity of the wrap increased the strength and the stiffness of the repaired columns. The effect of the fiber orientation on the strength and stiffness was coupled with the effect of the interfacial bonding. With perfect interfacial bonding, fibers in axial direction were more effective than those in hoop direction; with weak interfacial bonding, however, the effect of fiber orientation could be neglected.

Mirmiran et al. [9] focused on developing a nonlinear FE model for the analysis of FRP wrapped concrete. Solid elements were used for the concrete core, along with a non-associative Drucker-Prager (DP) [10] plasticity model, which takes into account the pressure sensitivity of the material. The parameters used to model the concrete included cohesion, angle of internal friction, and the dilatancy angle. The wrap was modeled by linear-elastic membrane shell elements. A parametric program was developed inside ANSYS software to automatically generate the mesh for various geometric shapes and material properties. The sensitivity analysis showed that response of FRP wrapped concrete can best be modeled by a zero dilatancy angle. It was shown that while the DP plasticity can be calibrated fairly well for predicting the axial stress-strain response, it does not properly establish the true dilation tendencies of the FRP wrapped concrete, simply because the DP model corresponds to an elastic-perfectly plastic material.

Above procedure was developed by Shahawy et al. [11] on CFRP wrapped concrete cylinders, and compared reasonably well with experimental results. It was concluded that the adhesive bond between concrete and the wrap would not significantly affect the confinement behavior. In experimental work, a total of 45 CFRP wrapped concrete cylinders were tested in uniaxial compression. Two concrete batches (normal and high strength) and five different numbers of wraps (from 1 to 5 layers) were used. The wrap significantly enhanced the strength and ductility of concrete by curtailing its lateral dilation.

Considering the previous researches on the fiber-wrapped concrete columns there are a number of issues that need to be addressed:

1. Based on the literature, the behavior of CFRP-wrapped concrete columns is not exactly clear in different conditions. What are the effects of the wrap thickness, fiber orientation, and concrete strength on strength and ductility of the columns?
2. There is not a consensus among researchers on the effects of interfacial bonding between the fiber-wrap and the concrete (Li et al. [6] and Shahawy et al. [11]). What is the exact behavior?
3. Is the ANSYS FE analysis with the DP plasticity an appropriate modeling for CFRP-wrapped concrete columns?
4. The dilatancy angle in the DP plasticity has been recommended equal to zero by Mirmiran et al. [9]. What is the best value of the dilatancy angle?

The present study is a numerical investigation on CFRP-wrapped concrete columns. In order to answer the above questions, a number of CFRP-wrapped concrete cylinders were modeled and analyzed by nonlinear FE method. Different fiber orientations, wrap thicknesses, interfacial bonding, concrete strength, and the DP plasticity parameters were considered. This parametric study is discussed in the following section.

## 3. Finite Element Analysis

### *3.1. Modeling*

The ANSYS FE software was used for 3D modeling of CFRP-wrapped concrete cylinders. All cylinders were 150 mm by 300 mm and were subjected to uniaxial compression. Due to symmetric geometry and loading, only 1/8 of each specimen (top quarter) is modeled (Fig. 1). The top quarter was made up three parts concrete core, FRP, and interfacial bonding between them. The concrete core and the FRP were built by first modeling 1/36th radial sector of the wrapped cylinder. The first sector of the wrap was meshed regularly with fifteen shell elements in axial direction. The top quarter of the concrete core was generated by repetition of this first sector and gluing the elements together as well as the wrap.

The concrete core was modeled using a special concrete element SOLID 65. This element is an 8-node solid brick element having three translation degrees of freedom per node. This element has crushing (compressive) and cracking (tensile) capabilities. The element can also accommodate plastic deformations and creep. The wrap was modeled by an 8-noded linear elastic SHELL99 element, which is a 3D layered shell element with six degrees of freedom per node. The element can accommodate 250 layers, variable thickness, orthotropic behavior, and large deflection.

The interfacial bonding between the wrap and the concrete core was modeled using a 2-noded CONTAC52 element, which is a 3D point to point contact element with three degree of freedom per node and an initial gap. This element is capable of supporting only compression in the direction normal to the surfaces and shear (coulomb friction) in the tangential direction. The element may be initially preloaded in the normal direction or it may be given a gap specification.  A specified stiffness acts in the normal and tangential directions when the gap is closed and not sliding. The normal stiffness should be based upon the stiffness of the surfaces in contact. The sticking stiffness represents the stiffness in the tangential direction when elastic coulomb friction is selected with a coefficient of friction as an input material property.

### *3.2. Material properties*

The characteristic response of fiber-wrapped concrete includes three distinct regions of un-cracked elastic deformations, crack formation and propagation, and plastic deformations. It is generally assumed that concrete behaves like an elastic-perfectly plastic material after reaching its maximum capacity, and that the failure surface is fixed in the stress space [9].

#### 3.2.1. Concrete

There are many constitutive models for confined concrete as a pressure and constraint sensitive material. In this study the DP plasticity model was employed, which assumes an elastic-perfectly plastic response. The DP model is a smooth circular cone along the hydrostatic axis in principal stress space. The DP cone for a triaxial state of stress in concrete is defined as

$$F = 3\beta\sigma_m + \sqrt{\frac{1}{2}\{S\}^T[M]\{S\}} - \sigma_y = 0, \qquad (1)$$

where $F$ is the yield function, $\sigma_m$ is the hydrostatic stress, $\{S\}$ is the deviatoric stress, $[M]$ is a special diagonal matrix (Eq. 2), $\sigma_y$ is the yield parameter of the material (Eq. 3), $\beta$ is a material parameter that are given by

$$[M]_{6\times 6} = \begin{bmatrix} I_{3\times 3} & 0 \\ 0 & 2I_{3\times 3} \end{bmatrix}, \tag{2}$$

$$\sigma_y = \frac{6C(\cos\phi)}{\sqrt{3}(3-\sin\phi)}, \tag{3}$$

$$\beta = \frac{2\sin\phi}{\sqrt{3}(3-\sin\phi)}, \tag{4}$$

where $I_{3\times 3}$ is the identify matrix, $C$ is the cohesion of the material (Eq. 5), $\phi$ is the internal friction angle of the material (Eq. 6) that have been suggested by Rochette and Labossiere [12] as

$$C = (f'_{co} - 5\sqrt{3})\frac{3-\sin\phi}{6\cos\phi}, \tag{5}$$

$$\phi = \sin^{-1}\left(\frac{3}{1+0.4f'_{co}/\sqrt{3}}\right), \tag{6}$$

where $f'_{co}$ is plain concrete strength in MPa.

The large volumetric dilation of plain concrete does not occur until the peak strength is approached. This fact will be used in the DP model. A linearly elastic element will be combined with the DP criterion in an elastic-perfectly plastic element, where the yield level depends on the level of confinement. Consider the plane where $\sigma_2 = \sigma_3$, shown in Fig. 2(a). Initially the element behaves perfectly linear. At point A the strength capacity under the current confining stresses is reached. However, the DP criterion still allows for an increase in the strength under increasing hydrostatic pressure, while plastic flow occurs on the failure surface. Plastic flow is controlled by a parameter $\phi_f$ called the dilatancy angle. It determines the flow rule and the amount of volumetric straining during the occurrence of plastic flow. [13]

According to the plastic theory, the plastic strain increment vector $d\bar{\varepsilon}_{pl}$ is perpendicular to the flow surface at any point. If the flow surface and the yield surface are assumed the same, the flow rule is called associated or, and $\phi_f$ is equal to $\phi$ (Fig. 2(b)). If flow surface and yield surface are not coincident the flow rule is non-associated, as presented in Fig. 2(c). Placing $d\bar{\varepsilon}_{pl}$ in the 3D strain space it can be seen that $\phi_f$ controls the volumetric behavior.

For selecting the dilatancy angle $\phi_f$, a sensitivity analysis was conducted in the next section and the stress-strain response was calibrated with experimental data. According to this analysis, the best value of the dilatancy angle was determined as one-half of internal friction angle ($\phi_f = 0.5\phi$).

3.2.1. FRP

The CFRP wrap was modeled as a linear orthotropic material. The mechanical properties of the wrap were calculated based on an experimental study reported by Sadeghian and Rahai [14]. In this experimental work, a number of CFRP coupons with a width of about 30 mm and a length of 250 mm were prepared in matrix and fiber directions with 1, 2, and 3 layers and tested under axial tension loading. The average mechanical and geometric properties of the coupons (per layer) are summarized in Table 1. The major and minor Poisson's ratios were assumed equal to 0.25 and 0.5 respectively. The major and minor shear modulus were calculated as 2500 MPa and 1333 MPa respectively by

$$G_{ij} = \frac{E_i E_j}{E_i + E_j + 2\nu_{ij} E_i}, \tag{7}$$

where $G_{ij}$ is the shear modulus, $E_i$ and $E_j$ are the elastic modulus, $\nu_{ij}$ is the Poisson's ratio, $i$ and $j$ are the fiber (major) direction and the matrix (minor) direction. The maximum tensile stress along fiber direction was selected as the failure criterion of specimens.

3.2-2. Interfacial bounding

The Interfacial bounding between FRP and concrete core was controlled with the friction coefficient in contact element, between 0 (unbounded) until 1 (bounded). In order to reduce time of analysis in fully bonded cases, the contact elements were removed and the adjacent nodes were constrained together.

*3.2. Boundary conditions and solution*

The symmetric condition was modeled on the three planes XY, XZ, and YZ (Fig. 1). Axial loading was applied on top surface of the concrete core using a user defined displacement increment. In order to simulate the rigid condition of loading plate in the testing machine, the displacement was applied to all nodes on the top surface of the concrete core, by constraining them together. The iterative Newton-Raphson procedure was used in the nonlinear FE analysis. When solution was converged at every sub-step, the outputs consisting of stresses, strains, deflections, and forces at critical locations were stored and processed to obtain axial and lateral stress-strain response, ultimate stress and strain, wrap forces, and ductility for the wrapped and plain specimens.

## 4. Results and discussion

### *4.1. Comparison with experimental results*

The validation of the FE analysis of fiber-wrapped concrete columns was controlled with an experimental study reported by Shahawy et al. [11] [15]. In this experimental study, laboratory tests were conducted on concrete cylinders 150 mm diameter by 300 mm height wrapped with CFRP composites under uniaxial compression. The specimens were used for the validation where concrete strength was 20.7 MPa (3 ksi) and Poisson's ratio was 0.12. The carbon wraps consisted of 1, 2, and 3 layers in hoop direction with thicknesses of 0.356 mm (0.014 in.), 0.584 mm (0.023 in), 0.813 mm (0.032 in) in sequence, and hoop modulus of elasticity of 82.8 GPa (12000 ksi), hoop strength 2277 MPa (330 ksi).

Fig. 3 shows a comparison of the stress-strain response of the control specimens obtained by the experiment and by the FE analysis. It is obvious that the FE analysis results are very close to the test results. This means that the FE modeling is validated by the test results. Hence, the FE modeling can be used to conduct a parametric analysis.

### *4.2. Sensitivity analysis*

It was mentioned before that the dilatancy angle $\phi_f$ is an important parameter in the DP model. In order to better understand the effect of the dilatancy angle on the stress-strain response of CFRP-wrapped concrete, a sensitivity analysis was carried out. Fig. 4 shows this effect, while the dilatancy angle was varied from zero to internal friction angle. As shown in the figure, the second slope of the response depends mainly on the dilatancy angle, and the best value is equal to one-half of internal friction angle.

*4.3. Parametric analysis*

To better understand the effects of modeling and physical parameters such as interfacial bonding, wrap thickness, fiber orientation, and concrete strength on behavior of CFRP wrapped concrete columns, a parametric analysis was conducted.

4.3.1. Interfacial bonding

In this section, the effect of interfacial bonding on the stress-strain response of CFRP wrapped columns was considered. The friction coefficient between FRP and concrete core was selected equal to 0, 0.25, 0.5, and 1. In extreme condition, fully interfacial bonding, the contact elements were removed and the adjacent nodes were constrained together. It can be observed that the interfacial bonding has not important effect on the stress-strain response (Fig. 5).

4.3.2. Wrap thickness

In this section, the effects of various wrap thicknesses on circular columns with concrete strength of 20 MPa are investigated. Fig. 6 shows comparison of FE analysis results for concrete columns with three different wrap layers 1, 2, and 3 in hoop direction (0.9 mm per layer). It is observed that the column with the 3 layers exhibits the highest axial stress carrying capacity as compared to other columns. The ultimate strain in all of cases is similar.

4.3.2. Fiber orientation

Fig. 7 shows the effect of the fiber orientation on the stress-strain response. In these specimens the concrete strength is 20 MPa and the wrap consists of two layers.

The fiber orientation ±45°, ±30°, ±15°, and 0°/0° were considered based on Fig. 8. It is observed that the hoop orientation of fibers (0°/0°) results in the largest gain in ultimate stress, while the angle orientation (±45°) leads to the largest ultimate strain (i.e. ductility).

4.3.3. Concrete strength

In this section, effect of the concrete strength was considered. The concrete strength was varied between 20 MPa and 40 MPa. The wrap thickness and fiber orientation were kept constant as two layers in hoop direction (0°/0°). Fig. 9 shows the stress-strain response of these specimens. It is observed that ultimate axial stress and strain are approximately similar, but slope of second part of the stress-strain curves are variable. In other word, the increase in stiffness is more pronounced for concrete having a lower unconfined compressive strength.

## 5. Conclusion

In this study, a finite element analysis was implemented on CFRP-wrapped confined concrete cylinders. An existing experimental study on CFRP-wrapped cylinders in the literature was employed to validate the numerical analysis. Based on the sensitivity analysis the best value of the dilatancy angle for concrete in Drucker-Prager model was determined as one-half of the internal friction angle. Based on the parametric analysis using the finite element modeling, the following conclusions can be drawn. The finite element analysis results showed substantial increase in the axial compressive strength and ductility of the CFRP-wrapped concrete cylinders as compared to the unconfined cylinders. The wrap thickness has a significant effect on the strength and stiffness of the columns. Increasing the wrap thickness can increase the strength and stiffness considerably. The gain in axial compressive strength was observed to be higher for lower strength concrete and the highest in the columns wrapped with the hoop orientation. The interfacial bonding has little effect on the stress-strain response.

**Acknowledgement**

The authors acknowledge the support of the Amirkabir University of Technology (Tehran Polytechnic), which enabled conducting this research.

**References**

[1] Teng JG, Lam L. Behavior and modeling of fiber reinforced polymer-confined concrete. J Struct Engng ASCE 2004;130(11):713-23.

[2] Parvin A, Jamwal AS. Effects of wrap thickness and ply configuration on composite-confined concrete cylinders. Compos Struct 2005;67(4):437–42.

[3] Lam L, Teng JG. Design-oriented stress-strain model for FRP-confined concrete. Constr Build Mater 2003;17(6&7):471–89.

[4] MSC.MARC. MSC Software Corporation, Palo Alto, CA; 2001.

[5] Parvin A, Jamwal AS. Performance of externally FRP reinforced columns for changes in angle and thickness of the wrap and concrete strength. Compos Struct 2006;73(4):451–7.

[6] Li G, Kidane S, Pang SS, Helms JE, Stubblefield MA. Investigation into FRP repaired RC columns. Compos Struct 2003;62(1):83–9.

[7] ANSYS user manual revision 5.4. Houston, PA; 1995.

[8] Willam KJ, Warnke EP. Constitute models for the triaxial behavior of concrete. Int. Assoc Bridge Struct Proc 1974; 19:1–30.

[9] Mirmiran A, Zagers K, Yuan W. Nonlinear FE modeling of concrete confined by fiber composites. FE Anal Des 2000;35(1):79-96.

[10] Drucker DC, Prager W. Soil mechanics and plastic analysis or limit design. Q Appl Math 1952;10(2):157-65.

[11] Shahawy M, Mirmiran A, Beitelman T. Tests and modeling of carbon-wrapped concrete columns. Compos Part B: Eng 2000;31(6-7);471-80.

[12] Rochette P, Labossiere P. A plasticity approach for concrete columns confined with composite materials. In: El-Badry MM editor. Proceedings Advanced Composite Materials in Bridges and Structures, CSCE, 1996. p. 359-66.

[13] Becque J. Analytical modeling of concrete columns confined by FRP, M.S. thesis, University of Manitoba, Canada, 2000.

[14] Sadeghian P, Rahai AR. Fiber orientation effects on tensile properties of CFRP composites in wrapped concrete columns, J Constr and Build Mat, (in review).

[15] Shahawy M, Beitelman T, Mirmiran A. Analysis and modeling of fiber-wrapped columns and concrete-filled tubes. Final Report, Structural Research Center, Florida Department of Transportation, Tallahassee, FL, 1998.

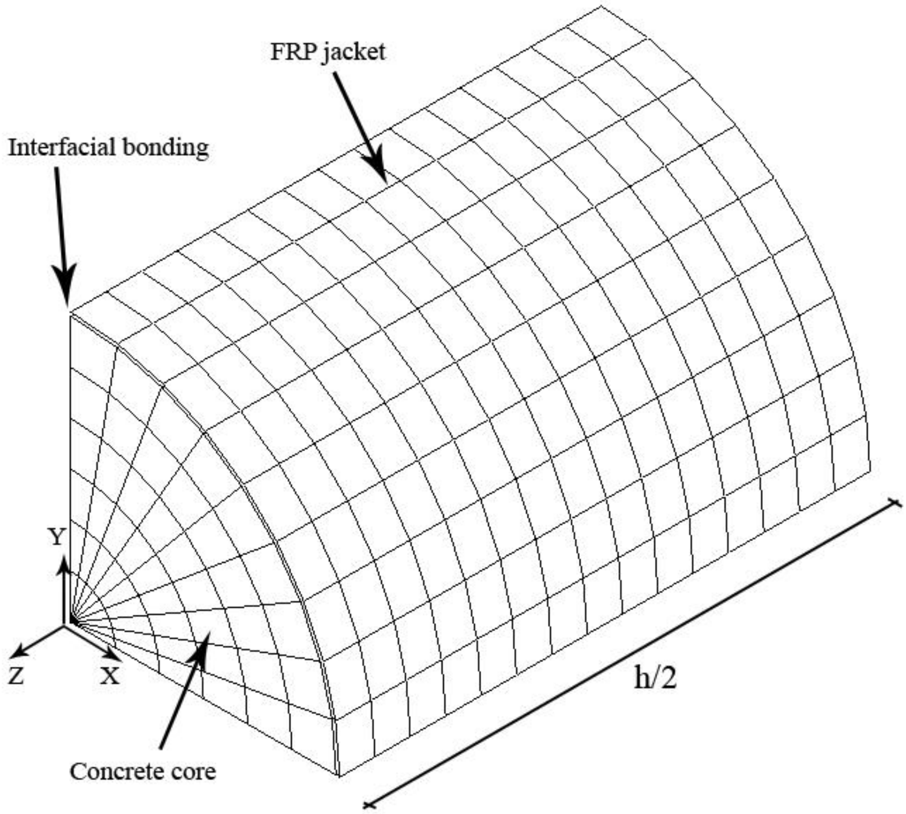


Fig. 1. FE modeling of 1/8 of each specimen (top quarter)

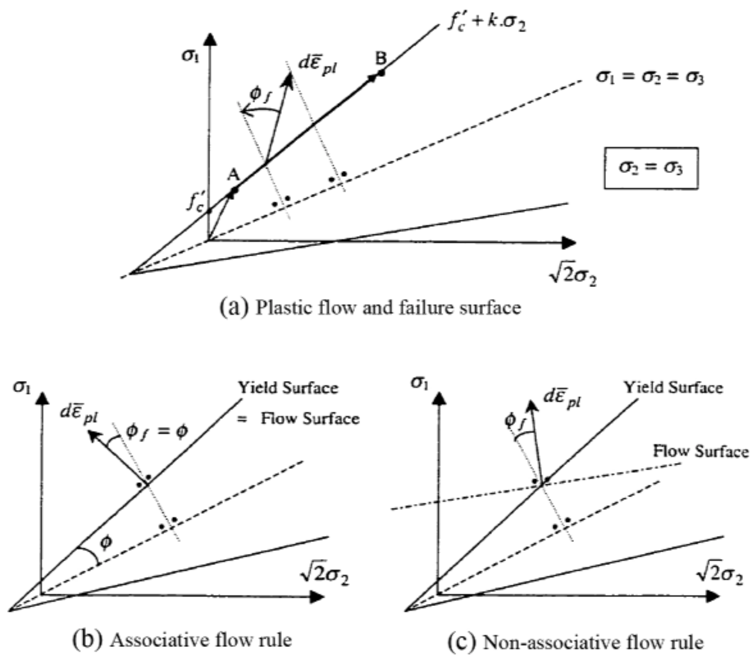


Fig. 2. Plastic flow and volumetric behavior in DP model [13]

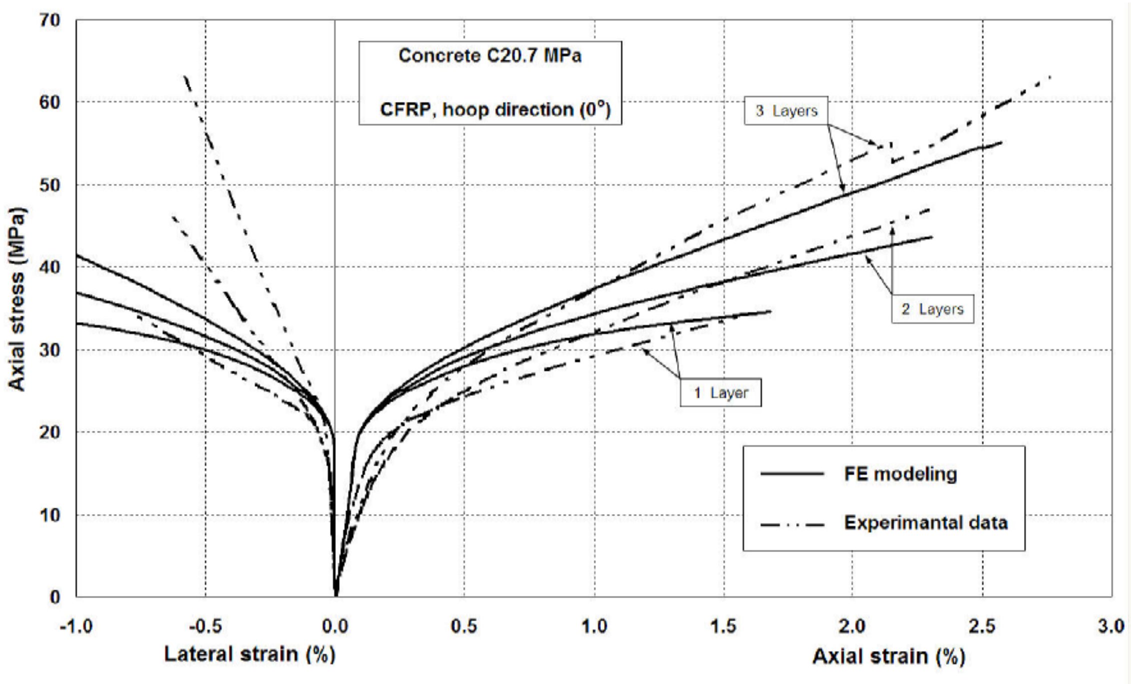


Fig. 3. Comparison of the FE modeling and experimental data

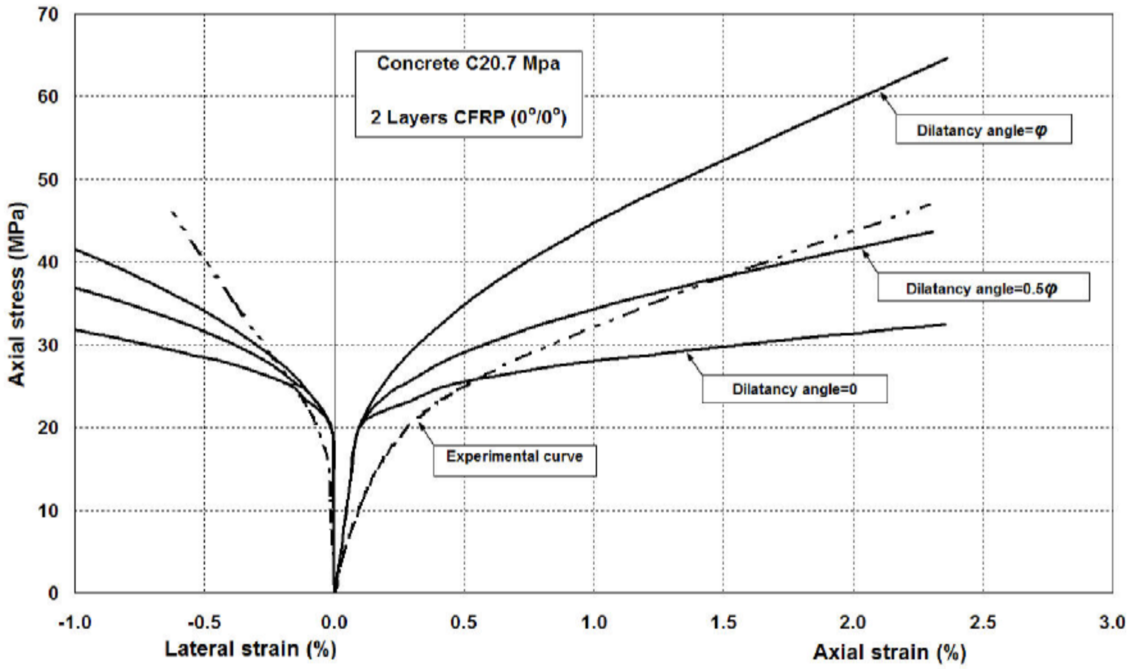


Fig. 4. Sensitivity analysis of the dilatancy angle on stress-strain response

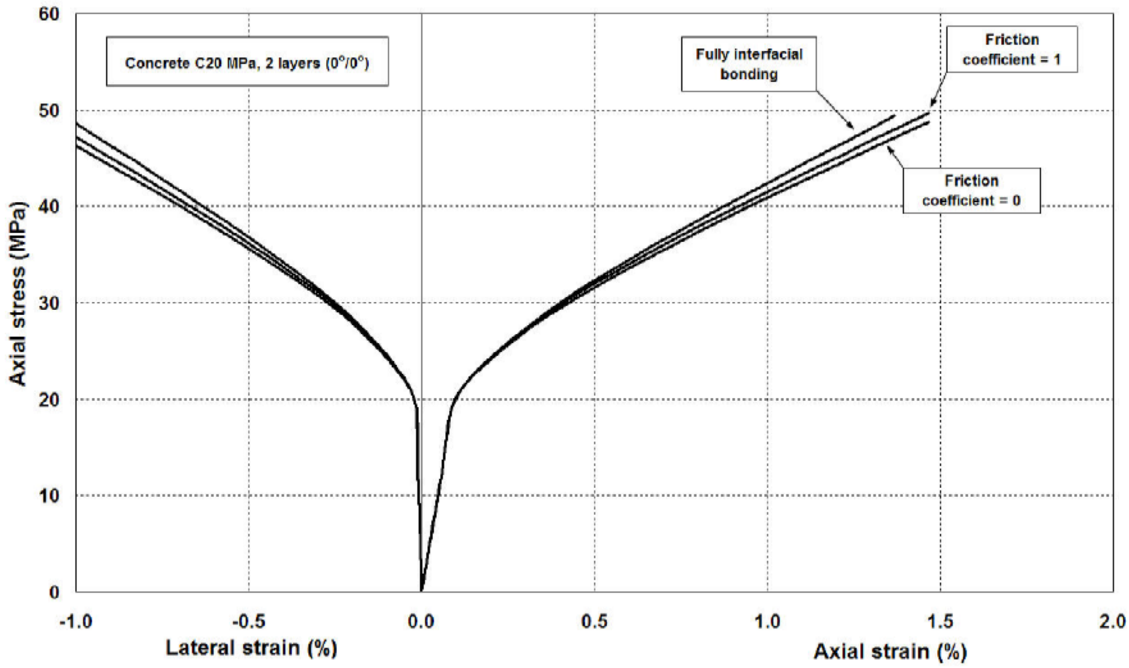


Fig. 5. Effect of interfacial bonding on stress-strain response

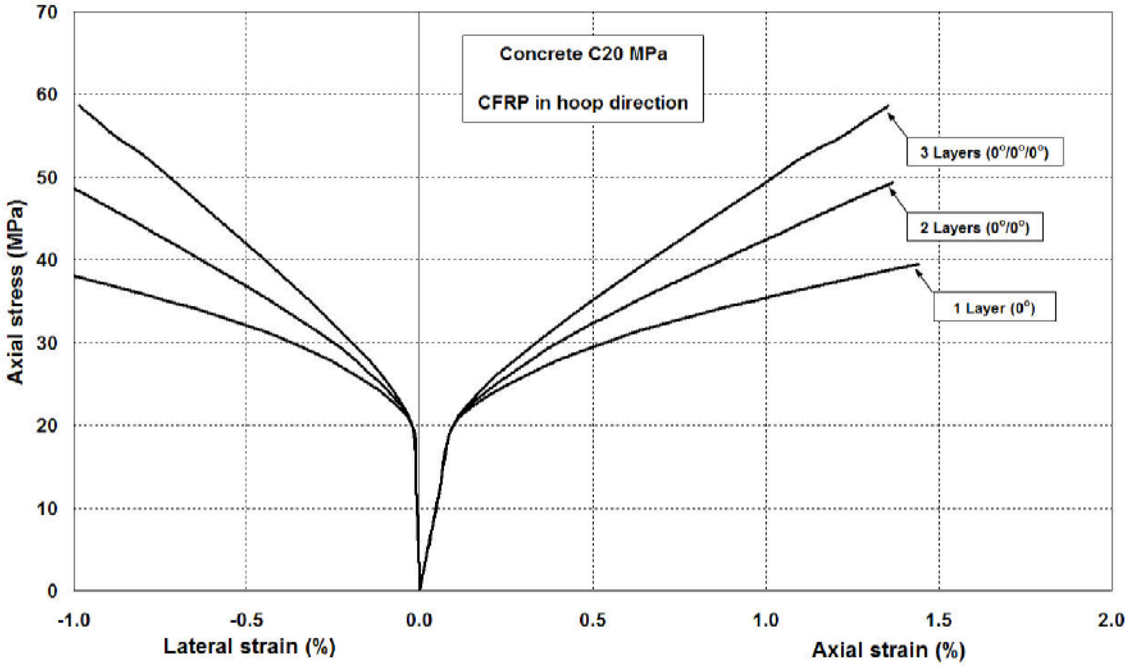


Fig. 6. Effect of wrap thickness on stress-strain response

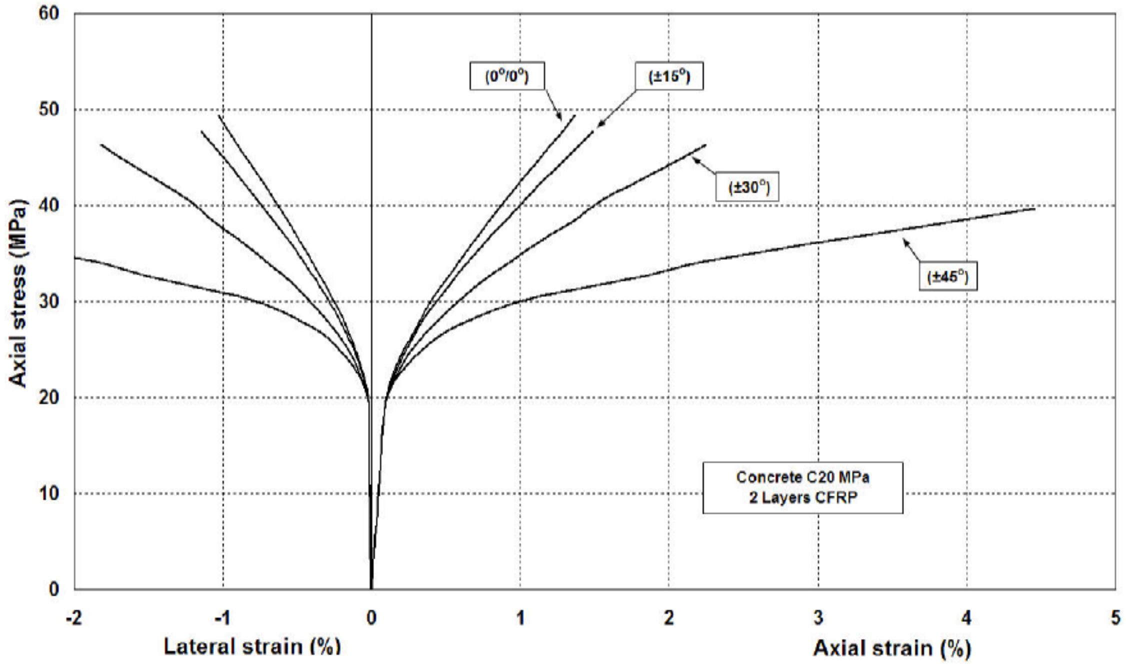


Fig. 7. Effect of fiber orientation on stress-strain response

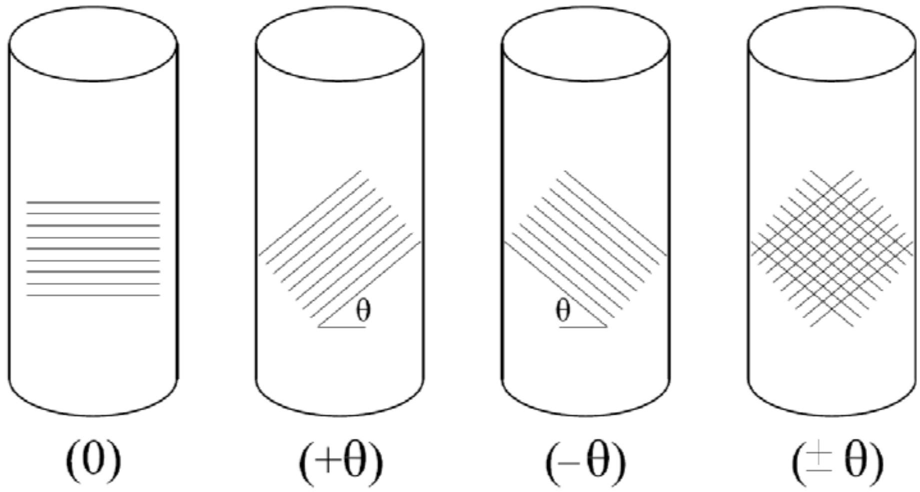


Fig. 8. Fiber orientation in CFRP-wrapped cylinders

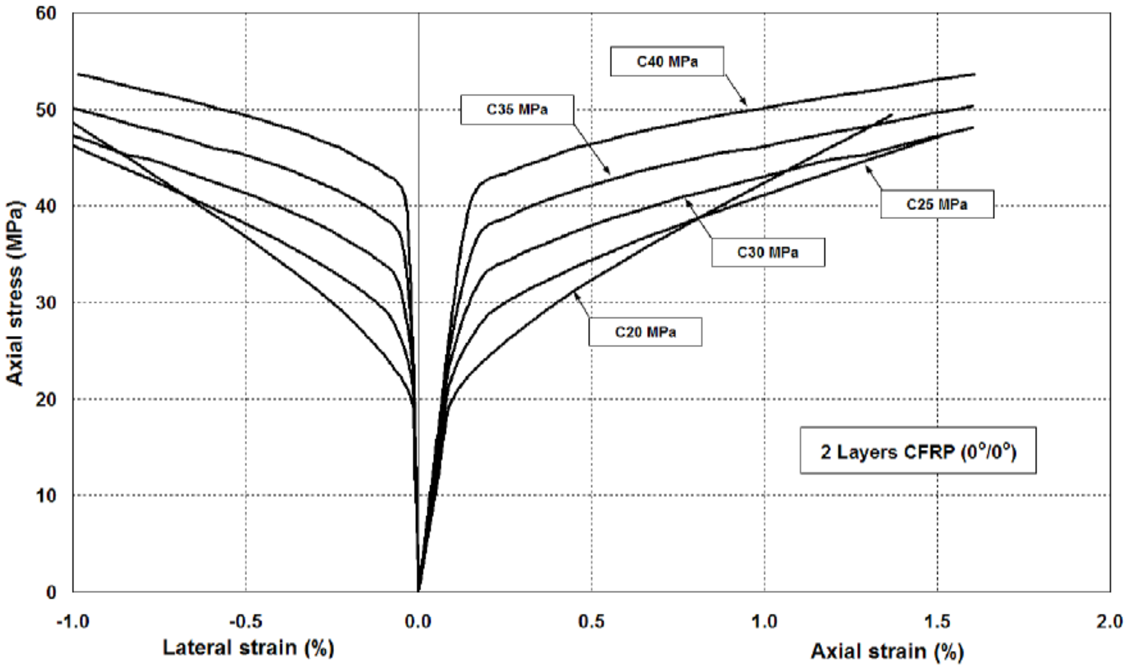


Fig. 9. Effect of concrete strength on stress-strain response

Table 1. Average results of CFRP coupon tension tests (per layer) [14]

| Test direction | Ultimate strength (MPa) | Elastic modulus (MPa) | Ultimate strain (%) | Thickness (mm) |
|---|---|---|---|---|
| Fiber direction ($0^o$) | 303 | 41000 | 0.74 | 0.90 |
| Matrix direction ($90^o$) | 29 | 4000 | 0.72 | 0.91 |

Note: 25.4 mm = 1 in, 1 MPa = 144.9 psi